Sensors and Actuators A 317 (2021) 112482

Contents lists available at ScienceDirect

Sensors and Actuators A: Physical

journal homepage: www.elsevier.com/locate/sna

A microfluidic device for blood plasma separation and fluorescence detection of biomarkers using acoustic microstreaming

Stanley C. Liu[a,b,*], Paul B. Yoo[c], Neha Garg[c], Abraham P. Lee[c], Suraiya Rasheed[a,*]

[a] University of Southern California, Los Angeles, CA, United States
[b] Arcadia High School, Arcadia CA, United States
[c] University of California Irvine, Irvine, CA, United States

ARTICLE INFO

Article history:
Received 1 October 2020
Received in revised form 9 November 2020
Accepted 24 November 2020
Available online 2 December 2020

Keywords:
Plasma separation
Acoustic microstreaming
Micromixer
Micropump
Biomarker detection

ABSTRACT

Human blood plasma contains numerous soluble, diffusible, and secreted biomarkers that are used for clinical diagnosis and prognosis of various diseases. However, the blood of some patients is hemolyzed rapidly due to the rupture of cell membranes and releases chemicals and biological molecules that yield false-positive fluorescence detection results due to autofluorescence. The standard method for plasma separation is centrifugation, which is difficult to be integrated with various methods for downstream biomarker detection. Herein, we report development of a novel microfluidic device that is integrated with multiple functionalities on a single disposable chip. Using the principle of bubble-induced acoustic microstreaming, we have tested whole blood controls spiked with fluorescently tagged antibodies to HIV-1 p24 protein and obtained ~ 31.8 % plasma yield with 99.9 % plasma purity within five minutes. The separated plasma was then routed to an integrated micro-mixing chamber and mixed with HIV-1 p24 antigen conjugated beads (10 μm diameter). The bound p24 antigen-antibody complexes were captured by acoustic microstreaming and detected using a fluorescence microscope. These experiments demonstrated a detection limit of ~17 pg/μL of p24 antibody in the plasma. The microfluidic device successfully separated plasma from the whole blood control using acoustic microstreaming and integrated with acoustic micro-pumping and micro-mixing for enrichment of biomarkers by mixing p24-bound beads with fluorescently tagged antibodies. The beads with antigen-antibody complexes were efficiently captured in a separate compartment for fluorescence microscopy and detection of biomarkers. Integration of multiple functionalities on a single disposable microfluidic chip can now facilitate rapid detection of biomarkers and be used for monitoring patients' specimen in real time.

1. Introduction

1.1. Plasma separation

Blood plasma is the most frequently used body fluid for the diagnosis and prognosis of disease-specific antigens, antibodies, fragments of DNA, RNA, and other markers that may be present in the plasma or other body fluids [1]. Plasma comprises approximately 55 % of a blood sample by volume while the remaining 45 % consists of Red Blood Cells (RBCs), White Blood Cells (WBCs), and platelets [1,2]. The blood cells are normally removed before diagnostic tests, because cell-membranes rupture easily during processing and release ammonia, potassium, glucose, and other chemical and biological molecules that hemolyze the blood, interfere with various tests downstream, and yield false-positive results [3–5]. Therefore, rapid separation of blood cells from plasma is one of the most vital steps in sample preparation for diagnostic tests. Centrifugation is one of the most common and efficient methods for plasma separation as it leverages centrifugal force to separate plasma from blood cells. While centrifugation is an efficient method for separating large or small volumes of blood, this process is time-consuming, requires bulky equipment, and is difficult to be integrated with downstream detection. We have therefore developed a small, cost-effective, and integrated device for acoustic microstreaming-based blood plasma separation and detection of fluorescently tagged antigen or antibodies.

* Corresponding authors at: University of Southern California, Los Angeles, CA, United States.
E-mail addresses: stanley_liu2003@yahoo.com (S.C. Liu), srasheed@med.usc.edu (S. Rasheed).

https://doi.org/10.1016/j.sna.2020.112482
0924-4247/

1.2. Microfluidics

Microfluidic technologies are emerging tools that can be used in well-controlled micro-scaled systems to achieve blood plasma separation [3–12]. These devices control the behavior of fluids within the unique channel designs, and can achieve a multitude of functionalities via electrical, acoustic, or magnetic forces. Microfluidic chips have the potential to provide more cost-effective, automated, and efficient functions that can easily be integrated and miniaturized to separate blood plasma [4–8].

Microfluidic filtration devices utilize well-designed pores smaller than the diameters of RBCs (6–8 μm) and WBCs (12–17 μm) to filter out blood plasma from the blood sample. Wang et al. have successfully developed a microfiltration device that used filter membranes with 0.4 μm diameter pores for plasma separation [4]. While this device was simple in design and easy to operate, the gradual buildup of blood cells around pores caused clogging and obstructed the flow of blood plasma. Although diluting blood with PBS (phosphate-buffered saline) in a 1:5 ratio to achieve 20 % hematocrit decreased the onset of clogging, this method is inefficient for collecting larger volumes of blood plasma. Most microfiltration devices were unable to process whole blood in high volumes and required low flow rates to avoid rupturing blood cell membranes as a result of high shear stress against the channel boundaries [4,5]. Low flow rates also increased the sample processing time and decreased the amount of blood plasma that could be extracted over a given period.

Lenshof et al. reported the use of ultrasonic standing wave (USW) to separate blood plasma in a microfluidic channel that is matched to a half wavelength width with a resonance around 2 MHz [13]. When a blood sample flowing through the channel was exposed to USW, acoustic forces moved all the blood cells to the pressure node located in the center of the channel, allowing plasma to exit through the side outlets. Several other microfluidic devices for blood plasma separation utilize hydrodynamic force [5–7,12], dielectrophoresis [8–10], and magnetic fields [11,12]. However, many of these devices yielded ~10 % blood plasma and are not as efficient as traditional bench-top centrifugation. Furthermore, many of them did not demonstrate integration of downstream biochemical analysis following plasma separation.

Micropumps are critical components in integrated microfluidic devices because they control the transportation of fluids to designated locations [14–17]. Conventional micropumps can be classified into two categories: membrane-actuated (mechanical) and non-membrane actuated. Membrane-actuated pumps are further divided into source-driven subtypes including piezoelectric, electrostatic, thermopneumatic, etc. Non-membrane pumping relies on electro-hydrodynamics, electro-osmosis, diffusion, traveling waves, surface tension, and other techniques. The majority of micropump technologies have complicated design and fabrication procedures, with an intricate operation and high cost. We have developed an effective acoustic microstreaming based micropump that is simple in design, easy to operate, and cost-effective for on-chip sample-to-answer biological analysis.

Micromixing of liquid solutions is also a critical component of many microfluidic systems that operate with multiple liquid reagents [16,17]. The flow of liquid solutions at microscopic level is inherently laminar, in which the Reynolds number is <1, and mixing is dominated by diffusion [17]. Turbulent flow-based mixing has previously been used in macro-scale fluidic systems but is not practical in microfluidic systems. Diffusion is highly inefficient in microfluidic systems, taking several hours to fully mix solutions [17,18]. Solutions with macromolecules (e.g., antibodies) or large particles (e.g., beads) and their subsequent low diffusion coefficients make diffusion-driven micromixing inefficient.

In this paper, we report the development of a microfluidic device for separation of blood plasma from blood cells, on-chip mixing for antigen-antibody binding, biomarker capture, and fluorescence detection of the biomarker. Blood plasma separation, biomarker capture, micro-pumping, and micro-mixing are based on the principle of bubble-induced acoustic microstreaming. Undiluted whole blood control samples spiked with fluorescently tagged HIV-p24 polyclonal antibodies was used to demonstrate the effectiveness of this novel device for plasma separation and immunoassay detection of HIV antibodies.

2. Design and fabrication

2.1. Acoustic microstreaming

The design of our device was based on the principle of acoustic microstreaming, in which the oscillation of an air bubble under an acoustic field forms a streaming flow [18–26]. Kolb et al. originally reported this phenomenon in 1956 during experiments applying various external forces on trapped air bubbles in aqueous solutions [20]. This principle was later observed when an acoustic field was created by a PZT (piezoelectric transducer), which acted upon an air bubble trapped by a cavity in a liquid phase [24]. The vibration of the PZT caused the bubble to oscillate stably and created fluidic streaming patterns (microstreaming vortex) around the air and liquid interface. At a certain frequency, acoustic microstreaming can be used to trap particles such as blood cells inside the microstreaming vortex whilst allowing blood plasma to flow downstream (Fig. 1a). The trajectory of a particle within a microstreaming vortex is largely dependent on its size and density. Patel et al. described how the streaming patterns around an air bubble produced closed-loop vortex [15]. Particles with varying diameters aligned their centers with different close-loop streamlines resulting in several size-dependent orbits [19]. This caused WBCs (12–17 μm diameter) to occupy smaller orbits closer to the microstreaming vortices and RBCs (6–8 μm diameter) occupy larger orbits. The nanometer-sized contents of blood plasma were easily displaced from the microstreaming vortex and flowed downstream whilst the large masses of blood cells were restricted from moving out of their size-dependent orbits. This resulted in the gradual separation of blood cells from the downstream plasma. As shown in Fig. 1(a), several rectangular lateral cavities with a width of 100 μm are positioned at a 15° angle from the microchannel. These cavities are used to trap air bubbles when the inlet solution enters the microchannel, pushing the excess air towards the outlet of the device. Each cavity produces an individual microstreaming vortex at the onset of an acoustic field.

Microstreaming vortices can also be used for enhancement of mixing between different liquid solutions in a microchamber [24]. As shown in Fig. 1(b), the bubble-trapped cavities are distributed on the cover layer of the microchamber. When exposed to an acoustic field, the air bubbles trapped in these cavities vibrate rapidly, generating microstreaming near each air bubble. The chamber has been designed specifically for close proximities between adjacent microstreaming vortices for rapid interaction of microstreaming, hence efficient micromixing. On-chip micromixing in the device was leveraged to bind fluorescently tagged target p24 antibodies with p24 antigens conjugated to polystyrene beads for fluorescent detection.

2.2. Device design

One of the main factors in optimizing plasma separation efficiency is based on the width of the microchannel. A narrow channel leads to the trajectories of particles in adjacent microstreaming

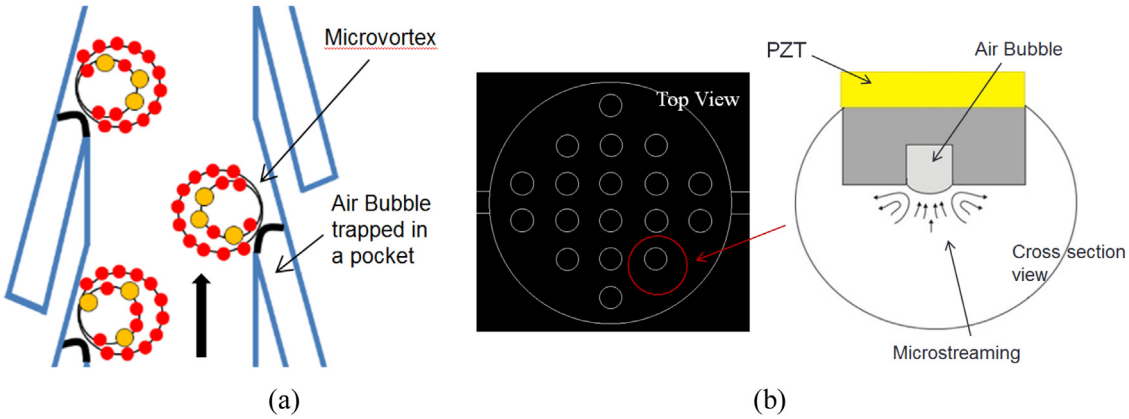

Fig. 1. Diagrams showing: (a) the blood cells (RBCs in red and WBCs in yellow) were trapped by air bubble induced acoustic microstreaming in a microfluidic channel with an array of lateral cavities; (b) acoustic microstreaming induced by the air bubbles that were trapped by the cavities machined in the cover layer of the chamber was used to enhance mixing in the chamber. (For interpretation of the references to colour in this figure legend, the reader is referred to the web version of this article).

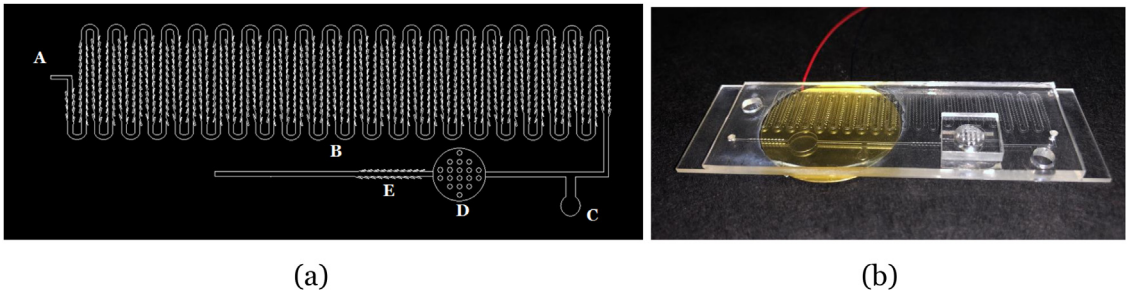

Fig. 2. (a) Schematic showing the design of the microfluidic device. (b) Photograph showing a Polydimethylsiloxane (PDMS) microchannel device assembled on a 75 mm × 25 mm glass slide and a PZT disk (yellow circle) superglued on the back of the glass slide. (For interpretation of the references to colour in this figure legend, the reader is referred to the web version of this article).

vortices intersecting with each other, displacing blood cells, and inhibiting the trapping of cells. In contrast, a wide microchannel under the laminar flow condition of microfluidic devices (Reynolds number <1) leads to particles passing through the middle of the channel without being trapped by the microstreaming vortices. In our previous study, a channel width of 500 μm was found to yield optimal plasma separation [26]. We therefore used this design for our new microfluidic device as shown in Fig. 2(a).

To test the device, an undiluted whole blood control sample spiked with fluorescently tagged HIV-p24 polyclonal antibodies was loaded into the inlet (Section A in Fig. 2(a)) of the plasma separation channel. Section B shows the plasma separation microchannel with 40 serpentine turns that increased throughput and maximized plasma separation efficiency. The serpentine microchannel is 50 μm deep, 500 μm wide, and 72 cm in total length. Hundreds of lateral cavities are angled at 15 degree along the channel wall to trap air bubbles when the blood solution flowed in the microchannel. These cavities have a width of 100 μm and a length of 500 μm. They are spaced 200 μm from each other.

When an acoustic field was produced by the PZT disk, the oscillation of the individual air bubbles in a forward motion caused the blood solution to flow downstream in Section B (Fig. 2(a)) and separated blood cells from the plasma solution. While the blood cells were retained inside the plasma separation channel (Section B), the pure plasma flowed into the downstream channel. Following that, polystyrene beads (10 μm dia.) conjugated to inactivated HIV-1 p24 antigens were loaded into the Section C inlet (Fig. 2(a)) and mixed with the separated plasma. Binding of the target p24 antibodies present in the plasma to the p24 antigen on the beads was enhanced through an acoustic mixing chamber with a diameter of 15 cm and several air bubbles trapped in vertical cavities (500 μm diameter and 500 μm depth) on the cover layer (Section D). The mixing formed antigen and antibody complexes, which flowed downstream towards a detection channel (Section E) where the 10 μm diameter polystyrene bead-conjugates were captured by bubble-induced acoustic microstreaming vortices and detected by fluorescence imaging.

2.3. Fabrication

The microfluidic device was fabricated using soft lithography technology [27]. The design of the device was developed using AutoCAD software and printed on a transparency as a mask by a printing company (CAD Art Services, Inc. Bandon, CA). This mask was then used to create a SU-8 mold by UV photolithography. SU-8 is an epoxy-based negative photoresist. The mold was created by using a 4″ diameter silicon wafer, SU-8 solution (Microchem, Newton, MA), and a spinner. The SU-8 solution was poured onto the wafer and spun at 5000 rpm on a spinner to achieve a 50 μm thick SU-8 layer. The wafer was then baked at 125 °C. The transparency mask was subsequently placed on the SU-8 and both were exposed to a UV light for 30 s. After development, the SU-8 wafer was baked for 1 min at 120 °C to complete the fabrication of the SU-8 mold. The microchannel pattern was then transferred from the SU-8 mold to Polydimethylsiloxane (PDMS) layer using the soft lithography technique [27]. PDMS pre-polymer (Sylgad 184 kit, Dow Corning, Midland, MI) was mixed and poured on top of the SU-8 Mold and baked at 75 °C for one hour on a hot plate. After baking, the finished PDMS was removed from the SU-8 mold, and inlet and outlet holes were made using a 3 mm diameter hole puncher. The PDMS was then placed on a glass slide and a 25 mm diameter PZT (APC Inter-

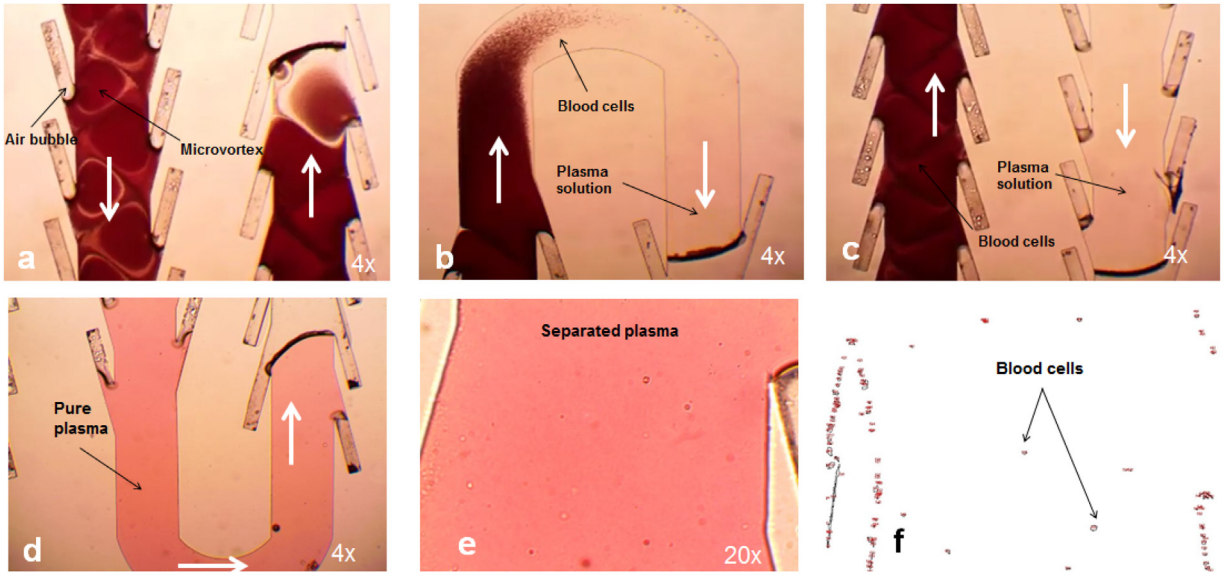

Fig. 3. Snapshots showing plasma extraction at various locations along the plasma separation microchannel. (a) Blood solution first entered the microchannel. (b–c) Blood cells were trapped by microstreaming vortices, eventually resulting in a plasma solution being separated from blood cells. (d–e) The pure plasma was observed at the end of the channel. (f) ImageJ software was used to analyze images to determine how many blood cells were contained in the plasma solution.

national, Mackeyville, PA) was attached to the bottom of the glass slide using a super glue (3 M, Saint Paul, MN).

The cover layer of the mixing chamber was manufactured in plastic (Polycarbonate) using a computer numerical control (CNC) machine. The top layer is a 1 mm thick polycarbonate (PC) that contains an array of vertical cavities, each with 0.5 mm diameter and 0.5 mm depth. The cover layer was bonded on the PDMS layer using a 0.1 mm thick double-sided pressure-sensitive adhesive tape (3 M, Saint Paul, MN) that was machined using laser cutting (Universal Laser System, Scottsdale, AZ).

3. Experimental setup

The microdevice was tested using human blood control samples (COULTER 5C Cell Control, Beckman Coulter, Brea, CA). During the tests, an undiluted blood control sample (50 μL) spiked with varying concentrations (10 pg/μL to 0.4 μg/μL) of FITC (Fluorescein isothiocyanate) tagged HIV-p24 antibodies (Thermo Fisher, Carlsbad, CA) was loaded into the inlet of the microdevice using a pipette. The HIV-p24 antibodies and antigens are major diagnostic tools for the diagnosis and prognosis of HIV-infection in humans [28]. A solution of inactivated p24 antigens (Abcam, Cambridge, MA) was also prepared by modifying biotin (Thermo Fisher, Carlsbad, CA) onto the surface of the antigens. 10 μm polystyrene beads coated with streptavidin (Spherotech, Lake Forest, IL) were then centrifuged with the biotinylated p24 antigens at 10,000 RPM for 10 min to conjugate the p24 antigens with the polystyrene beads.

Once the blood was loaded in the inlet port of the microchannel, a function generator (Agilent, Palo Alto, CA) connected to the PZT disk applied a square wave current with a current amplitude of 5 mA and a frequency of 16 kHz onto the device. A TS200 modulated power supply amplifier (Accel Instruments Corp., Irvine, CA) was used to increase the voltage to 30 V_{pp} to optimize plasma separation efficiency. Application of an acoustic field onto the trapped air bubbles caused the formation of individual microstreaming vortices around individual air bubbles and the fluid transport of the solution downstream. The separated plasma containing target p24 antibodies flowed into the mixing chamber, a 30 μL solution of p24 antigens conjugated to 10 μm polystyrene beads were loaded into the device at the section C inlet (Fig. 2a). The function generator was then adjusted to an amplitude of 5 mA and a frequency of 9 kHz for 3 min to maximize the efficiency of mixing and enhance binding between the inactivated p24 antigens and target p24 antibodies. Next, the mixed solution was transported into the detection channel where the function generator was adjusted to the initial frequency of 16 kHz and the conjugated protein complexes were captured and fluorescently imaged under a microscope. A PBS wash buffer was introduced from the Section C loading port (Fig. 2a) to wash the beads to remove extra, non-bound antibodies from the capture/detection chamber prior to detection of antigen-antibody complexes.

Images of the target p24 antibodies bound to the p24-antigen on microbeads were captured using a fluorescence microscope (Olympus, Tokyo, Japan) with an excitation filter wavelength of 495 nm and an emission filter wavelength of 519 nm. ImageJ software (National Institutes of Health, Bethesda, Maryland) was used to analyze 20x magnification pictures of the separated plasma to count the number of blood cells present and analyze separation efficiency of the device. ImageJ was also used to analyze the fluorescence images and determine the sensitivity of p24 antibody detection.

4. Results and discussion

4.1. Plasma separation

We have successfully separated whole blood plasma from cells using acoustic microstreaming around the air bubbles retained in the lateral cavities in the plasma separation microchannel (Fig. 3a–c). Individual air bubbles produced individual microstreaming vortices, attracting and trapping blood cells within close-loop orbits due to their large mass. The continuous trapping of blood cells and downstream flow of the solution subsequently resulted in plasma separation, with channel sections further downstream having significantly fewer cell concentrations compared to previous sections (Fig. 3b and c). The bulk of blood cells were separated from the plasma solution after several serpentine turns (Fig. 3d and e).

With the use of multiple lateral cavities along a lengthy serpentine microchannel, we were able to trap blood cells and achieve a

pure plasma solution at the end of the plasma separation channel, containing the target p24 antibodies. An important step to determine the purity of plasma after separation was to analyze the plasma images and count the blood cells contained in the plasma. Manual counting of blood cells under a microscope is labor-intensive, time-consuming, and susceptible to human error due to the tedious nature of this process. We used an image analysis software (ImageJ) which analyzed the acquired images at 20x magnification of the plasma and counted cells automatically (Fig. 3e). The analysis of microscopic images to recognize blood cells was conducted in a four-step process: pre-processing, image segmentation, feature extraction, and classification [29]. The pre-processing stage included image enhancement of the acquired image and was performed to prepare the image for the vital segmentation stage. Individual objects of interest were then separated from the background in the segmentation process. During the post-processing stage, objects that were previously segmented were tagged with unique labels (such as WBC, RBC, etc.), paramount to the counting of the blood cells (Fig. 3f). The final count of different labels resulted in the number of cells present in each given image.

To obtain the average cell count, 20 different photos were captured at the end of the plasma separation microchannel from the same blood control sample at 20x magnification. All images were then processed by ImageJ. This process was repeated across 30 experiments to determine the average separation efficiency. The ratio of the blood cells found in 1 μL of the extracted plasma solution over the average number of blood cells (4.8 million) in 1 μL of the whole blood determined the separation efficiency in each of the 30 experiments. The average plasma purity obtained by this device was 99.9 %. The yield of the plasma separation was determined by measuring the ratio of the total amount of plasma extracted over the total amount of input blood samples. The plasma yield of our device was 31.8 %, which was lower than the 55 % yield of a benchtop centrifuge, but higher than the yield of many other microfluidic-based plasma separation devices [3]. About 15.9 μL of plasma was separated from the initial 50 μL blood sample. The volume of extracted plasma was proportional to the device dimensions. It is expected that the plasma separation can be scaled up by increasing the separation channel length.

The acoustic microstreaming device displayed advantages over the other plasma separation microfluidic techniques. For example, the plasma separation microchannel of our device has a large width (i.e., 500 μm) and does not clog by the blood samples, whereas the other plasma separation devices rely on particle retention using a microfilter structure or a bead packed microchannel, which clogs easily [3,4]. As compared to hydrodynamic effects and dielectrophoresis [8–12], acoustic microstreaming filters through

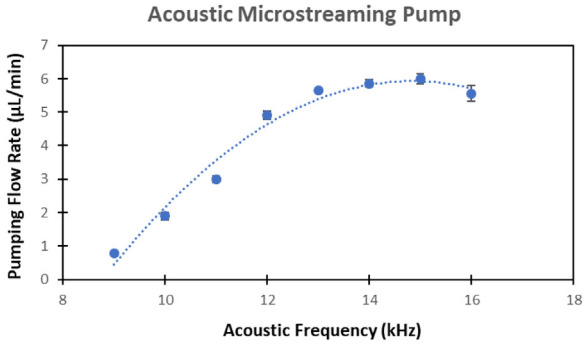

Fig. 4. Diagram showing the flowrate of the acoustic microstreaming based micropump as a function of acoustic frequency. The maximum flowrate of 6 μL/min was achieved at a frequency of 15 kHz and a voltage of 30 V_{pp}.

every single cell within a single pass of the channel, resulting in highly purified plasma and high cell separation efficiency. As compared to ultrasonic standing wave (USW) acoustophoresis, which relies on high acoustic force and energy to concentrate blood cells into a band sufficiently narrow to enable separation [13], bubble-induced acoustic microstreaming requires less driving voltage to the piezoceramic transducer and thus produces minimal temperature increase in the device. Moreover, an acoustophoresis device needs an additional pump to move the blood solution in the microchannel whereas bubble-induced acoustic microstreaming provides plasma separation and liquid pumping simultaneously.

4.2. Acoustic micropump

Acoustic microstreaming has been previously shown to achieve a high degree of fluid transport [15,25]. The positioning of the air cavities diagonally from the main channel with an angle of 15 degree and the initial movement of oscillating bubbles acted as a continuous actuator to move fluid forward in the device. This was explored in depth by Patel et al., who hypothesized that fluid transport was caused by the bulk flow of fluid between the interface of the air bubbles and microstreaming vortices [15]. Particles smaller than 2x the length of the gap between interfaces could flow downstream whilst the larger particles remained in their closed-loop vortices. The pump rate of our device was measured as a function of the acoustic frequency as shown in Fig. 4. A flowrate as high as 5.8 μL/min was achieved at a frequency of 16 kHz and a voltage of 30 V_{pp}. The integration of an acoustic micropump in our device is highly advantageous, because it does not require any

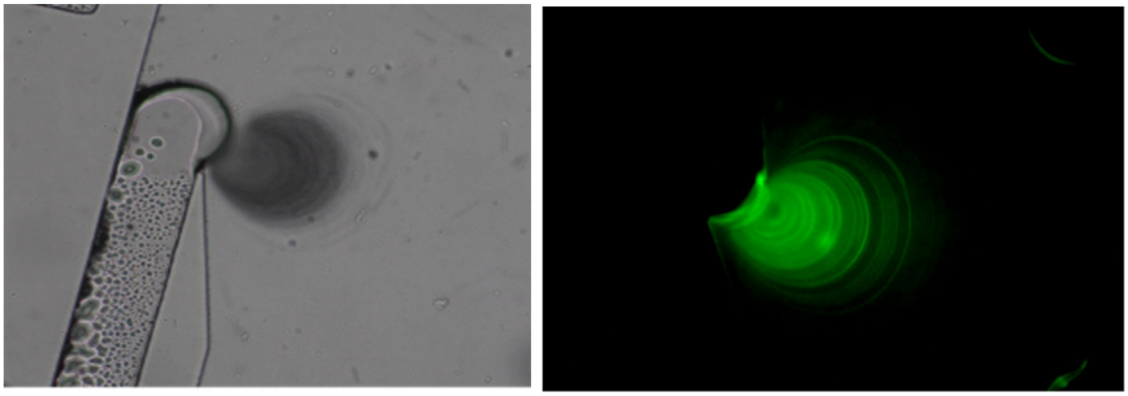

Fig. 5. Images showing the biomarker/beads captured by the microstreaming vortex in the capture channel. The fluorescent image (b) indicates that the target p24 antibodies were captured.

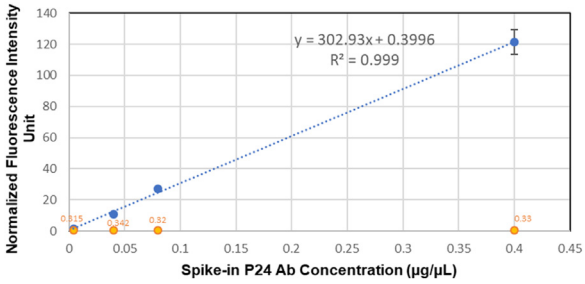

Fig. 6. The fluorescent signal analysis demonstrates the linear dynamic range of the p24 antibody detected using the integrated microfluidic device. Each data point (blue dot) represents the mean of the normalized fluorescent intensities for the spiked-in p24 antibody in separated plasma against the corresponding concentrations (0.004 μg/μL to 0.4 μg/μL). Error bars indicate the standard deviation across the detection channel at each data point. The yellow-dot data points at bottom represent the mean of negative control signals. (For interpretation of the references to colour in this figure legend, the reader is referred to the web version of this article).

external pumping equipment and the simple design of the micropump makes it easy to fabricate and operate.

4.3. Fluorescent biomarker detection

The target, HIV-p24 antibodies fluorescently tagged with FITC in the separated plasma were mixed and bound with polystyrene beads (10 μm dia.) conjugated to p24 antigens to form protein complexes. The protein complexes were then captured by bubble-induced acoustic microstreaming vortices due to the large size of the polystyrene beads and subsequently detected by fluorescence imaging in the detection channel (Fig. 5). The fluorescence images were analyzed by ImageJ to obtain the fluorescence intensity of the captured p24 antibodies. This process was repeated over 24 sets of data with spiked p24 antibody concentrations ranging from 0.004 μg/μL to 0.4 μg/μL. The fluorescent signals were measured on all the trapping microvortices in the detection channel. As shown in Fig. 6, each data point is the mean of the normalized fluorescence intensities for the spiked-in p24 antibody in separated plasma against the corresponding concentrations over 24 sets of data. The fluorescent intensity signal of the p24 antibody detected in the microdevice was linear across the range of p24 antibody concentrations (0.004–0.4 μg/μL), with a standard curve R^2 value of 0.999. In determining the cutoff for sensitivity or LLD (lower limit of detection), signal was considered significant if greater than three standard deviations above the average of the negative control signals. Our further studies with low spiked-in p24 antibody concentrations (~ 10 pg/μL) showed that the detection limit of our device was 17 pg/μL, which is higher than the p24 detection limit (10 pg/mL) of the fourth-generation HIV enzyme-linked immunosorbent assay (ELISA) immunoassays [30], indicating that there is a room for improvement of the detection sensitivity of our device.

5. Conclusion

We have successfully developed a microfluidic device for separation of blood plasma, antigen/antibody binding, biomarker capture, and fluorescence detection of the biomarker. Blood plasma was separated from the whole blood control sample using acoustic microstreaming with 31.8 % plasma yield and 99.9 % plasma purity. Acoustic microstreaming showed superior advantages over the other plasma separation techniques, including: 1) simple device design; 2) easy to fabricate and operate; 3) no issue of cell clogging; and 4) easy to integrate with other downstream components. In addition, acoustic microstreaming can be used as a micropump to achieve a flowrate of ~5.8 μL/min in a microchannel. Acoustic microstreaming can also be used as a micromixer to enhance antigen/antibody mixing and binding. The demonstration of the detection of ~17 pg/μL of target HIV p24 antibodies from a whole blood control sample using this microfluidic device indicates that acoustic microstreaming can be used to integrate multiple functionalities on a single disposable microfluidic chip to facilitate rapid detection of biomarkers and monitoring patients' specimen in real time.

CRediT authorship contribution statement

Stanley C. Liu: Conceptualization, Data curation, Formal analysis, Investigation, Methodology, Project administration, Resources, Software, Validation, Writing - original draft. **Paul B. Yoo:** Supervision, Writing - review & editing. **Neha Garg:** Supervision, Writing - review & editing. **Abraham P. Lee:** Supervision, Writing - review & editing. **Suraiya Rasheed:** Supervision, Writing - review & editing.

Declaration of Competing Interest

The authors report no declarations of interest.

Acknowledgement

We thank Dr. Robin Liu at Hochuen International Corp. for his continuous help and support in the design of the devices.

References

[1] W.S. Mielczarek, E.A. Obaje, T.T. Bachmann, M. Kersaudy-Kerhoas, Microfluidic blood plasma separation for medical diagnostics: is it worth it? Lab Chip 16 (2016) 3441.
[2] D.M. Harmening, Clinical Hematology and Fundamentals of Hemostasis, F. A. Davis Co, Philadelphia, 1992.
[3] S. Tripathi, Y.V.B.V. Kumar, A. Prabhakar, S.S. Joshi, A. Agrawal, Passive blood plasma separation at the microscale: a review of design principles and microdevices, J. Micromech. Microeng. 25 (2015) 83001–83025.
[4] S. Wang, D. Sarenac, M.H. Chen, S.-H. Huang, F.F. Giguel, D.R. Kuritzkes, U. Demirci, Simple filter microchip for rapid separation of plasma and viruses from whole blood, Int. J. Nanomed. 7 (2012) 5019–5028.
[5] M. Kersaudy-Kerhoas, E. Sollier, Micro-scale blood plasma separation: from acoustophoresis to egg beaters, Lab Chip 13 (17) (2013) 3323–3346.
[6] S. Tripathi, Y.V.B. Kumar, A. Agrawal, A. Prabhakar, S.S. Joshi, Microdevice for plasma separation from whole human blood using biophysical and geometrical effects, Nature 6 (2016) 26749.
[7] H.W. Hou, A.A.S. Bhagat, W.C. Lee, S. Huang, J. Han, C.T. Lim, Microfluidic devices for blood fractionation, Micromachines 2 (2011) 319–343.
[8] C. Szydzik, K. Khoshmanesh, A. Mitchell, C. Karnutsch, Microfluidic platform for separation and extraction of plasma from whole blood using dielectrophoresis, Biomicrofluidics 9 (2015), 064120.
[9] A. Anas, S. Ion, B. Rama, M. Ari-Nareg, Interdigitated comb-like electrodes for continuous separation of malignant cells from blood using dielectrophoresis, Electrophoresis 32 (2011) 1327–1336.
[10] M.S. Pommer, Y. Zhang, N. Keerthi, D. Chen, J.A. Thomson, C.D. Meinhart, H.T. Soh, Dielectrophoretic separation of platelets from diluted whole blood in microfluidic channels, Electrophoresis 29 (2008) 1213–1218.
[11] K.-H. Han, A.B. Frazier, Paramagnetic capture mode magnetophoretic microseparator for high-efficiency blood cell separations, Lab Chip 6 (2006) 265–273.
[12] H.K. Seo, Y.H. Kim, H.O. Kim, Y.J. Kim, Hybrid cell sorters for on-chip cell separation by hydrodynamics and magnetophoresis, J. Micromech. Microeng. 20 (2010), 095019.
[13] A. Lenshof, A. Ahmad-Tajudin, K. Järås, A.M. Swärd-Nilsson, L. Aberg, G. Marko-Varga, J. Malm, H. Lilja, T. Laurell, Acoustic whole blood plasmapheresis chip for prostate specific antigen microarray diagnostics, Anal Chem. 81 (15) (2009) 6030–6037.
[14] I. Dimov, L. Basabe-Desmonts, J. Garcia-Cordero, B. Ross, A. Ricco, L. Lee, Stand-alone self-powered integrated microfluidic blood analysis system, Lab chip 11 (2011) 845–850.
[15] M. Patel, I. Nanayakkara, M. Simon, A. Lee, Cavity-induced microstreaming for simultaneous on-chip pumping and size-based separation of cells and particles, Lab Chip 14 (2014) 3860–3872.
[16] A. Manz, N. Graber, H.M. Widmer, Miniaturized total chemical analysis systems: a novel concept for chemical sensing, Sens. Actuators, B 1 (1990) 244–248.
[17] R.H. Liu, A. Lee, Integrated Biochips for DNA Analysis, Springer, New York, 2007.

[18] R.H. Liu, J. Yang, R. Lenigk, J. Bonanno, P. Grodzinski, Self-contained, fully integrated biochip for sample preparation, PCR amplification, and DNA microarray detection, Anal. Chem. 76 (2004) 1824–1832.
[19] N. Garg, T.M. Westerhof, V. Liu, R. Liu, E.L. Nelson, A.P. Lee, Whole-blood sorting, enrichment and in situ immunolabeling of cellular subsets using acoustic microstreaming, Microsyst. Nanoeng. 4 (2018) 17085.
[20] J. Kolb, W.L. Nyborg, Small-scale acoustic streaming in liquids, J. Acoustical Soc. Am. 28 (1956) 1237–1242.
[21] W.L. Nyborg, Acoustic streaming near a boundary, J. Acoustical Soc. Am. 30 (1958) 329–339.
[22] M. Wiklund, R. Green, M. Ohlin, Acoustofluidics 14: applications of acoustic streaming in microfluidic devices, Lab Chip 12 (2012) 2438–2451.
[23] S.J. Lighthill, Acoustic streaming, J. Sound Vib. 61 (1978) 391–418.
[24] R.H. Liu, J. Yang, M.Z. Pindera, M. Athavale, P. Grodzinski, Bubble-induced acoustic micromixing, Lab Chip 2 (2002) 151–157.
[25] A.R. Tovar, M.V. Patel, A.P. Lee, Lateral air cavities for microfluidic pumping with the use of acoustic energy, Microfluid. Nanofluid. 10 (2011) 1269–1278.
[26] S. Liu, N. Garg, A.P. Lee, A microfluidic device for plasma separation from whole blood samples using bubble-induced acoustic microvortex, in: Proceedings of the 22nd International Conference on Miniaturized Systems for Chemistry and Life Sciences, Kaohsiung, Taiwan, 2018, pp. 2367–2368, 11-15 November.
[27] Y. Xia, G.M. Whitesides, Soft lithography, Angew. Chem. Int. Ed. Engl. 37 (1998) 551–575.
[28] S. Rasheed, Molecular methods in human retrovirology, in: K.W. Adolph (Ed.), Methods in Molecular Genetics, Vol. 4, Academic Press Inc., Orlando, Florida, 1996, pp. 111–166.
[29] H. Refai, L. Li, T.K. Teague, R. Naukam, Automatic count of hepatocytes in microscopic images, Proc. Int'l Conf. on Image Processing, 2, Sept (2003) 1101–1104.
[30] M.S. Cohen, C.L. Gay, M.P. Busch, F.M. Hecht, The detection of acute HIV infection, J. Infect. Dis. 202 (2010) S270–S277.

Biographies

Stanley C. Liu is currently a student at Arcadia High School, Arcadia, CA, USA. He is doing part-time research on microfluidics at both University of Southern California and University of California at Irvine.

Paul B. Yoo is currently a Ph.D. student at University of California at Irvine, working on microfluidics. He received his BS in Engineering Physics from University of California at San Diego. He was an engineer at Samsung Electronics America in 2012–2016.

Neha Garg received her Ph.D. in Biomedical Engineering at University of California at Irvine in 2019, and BS in Biotechnology and Biochemical Engineering at Indian Institute of Technology in 2014. She is currently a Staff Scientist at Thermo Fisher Scientific. She works on microfluidics, microarrays, molecular biology, bio-assay development, and product development.

Abraham (Abe) P. Lee is the William J. Link Professor of the Biomedical Engineering (BME) Department at the University of California, Irvine. He is the Director of the NSF I/UCRC "Center for Advanced Design & Manufacturing of Integrated Microfluidics" (CADMIM). He started his appointment as Editor-in-Chief for the Lab on a Chip journal in January 2017. He owns more than 40 issued US patents and has published more than 100 journal articles and awarded the 2009 Pioneers of Miniaturization Prize and is an elected fellow of the American Institute of and Medical and Biological Engineering and the American Society of Mechanical Engineers.

Suraiya Rasheed is a Professor and Director of Viral Oncology and Proteomics Laboratory in the Department of Pathology at the Keck School of Medicine, University of Southern California, Los Angeles, USA. She has graduated with honors and received her first Ph.D. from Osmania University, Hyderabad, India and second Ph.D. from London University. She has also served numerous national and international Advisory Committees including Study Sections of the National Cancer Institute, National Institute of Allergy and Infectious Diseases, Antiviral Drug Development and Drug Screening Programs for AIDS and Abstract Reviewing Committee for the International AIDS Society's conferences. She is a Fellow of Royal College of Pathologists, London.